Miscible density fingering of chemical fronts in porous media: Nonlinear simulations

A. De Wit[a)]
Service de Chimie Physique and Centre for Nonlinear Phenomena and Complex Systems, CP 231, Université Libre de Bruxelles, 1050 Brussels, Belgium

(Received 19 May 2003; accepted 5 October 2003; published online 5 December 2003)

Nonlinear interactions between chemical reactions and Rayleigh–Taylor type density fingering are studied in porous media or thin Hele-Shaw cells by direct numerical simulations of Darcy's law coupled to the evolution equation for the concentration of a chemically reacting solute controlling the density of miscible solutions. In absence of flow, the reaction-diffusion system features stable planar fronts traveling with a given constant speed v and width w. When the reactant and product solutions have different densities, such fronts are buoyantly unstable if the heavier solution lies on top of the lighter one in the gravity field. Density fingering is then observed. We study the nonlinear dynamics of such fingering for a given model chemical system, the iodate-arsenious acid reaction. Chemical reactions profoundly affect the density fingering leading to changes in the characteristic wavelength of the pattern at early time and more rapid coarsening in the nonlinear regime. The nonlinear dynamics of the system is studied as a function of the three relevant parameters of the model, i.e., the dimensionless width of the system expressed as a Rayleigh number Ra, the Damköhler number Da, and a chemical parameter d which is a function of kinetic constants and chemical concentration, these two last parameters controlling the speed v and width w of the stable planar front. For small Ra, the asymptotic nonlinear dynamics of the fingering in the presence of chemical reactions is one single finger of stationary shape traveling with constant nonlinear speed $V>v$ and mixing zone $W>w$. This is drastically different from pure density fingering for which fingers elongate monotonically in time. The asymptotic finger has axial and transverse averaged profiles that are self-similar in unit lengths scaled by Ra. Moreover, we find that W/Ra scales as $Da^{-0.5}$. For larger Ra, tip splittings are observed. © *2004 American Institute of Physics.*
[DOI: 10.1063/1.1630576]

I. INTRODUCTION

Chemical reactions can interact with hydrodynamic fingering instabilities and affect the stability properties as well as the nonlinear spatiotemporal dynamics of the system. Several works have focused in this respect on the interplay between viscous fingering and chemical reactions in porous media or Hele-Shaw cells. Ortoleva and co-workers have shown theoretically that, in porous media, chemical dissolution of the porous matrix can change its permeability giving rise to a hydrodynamic fingering instability.[1] In Hele-Shaw cells, the influence of chemistry on immiscible viscous fingering patterns has experimentally been strikingly evidenced by Hornof and co-workers[2] and more recently by Sastry *et al.*[3] and by Fernandez and Homsy.[4] In the latter case, surface tension effects are dominant. For miscible systems, experiments on viscous fingering in reactive systems have addressed the effect of the variation of reactant concentrations and of the finger pattern on the spatial distribution of chemical species showing that the flow can drastically influence the reaction.[5] However, in these systems, the chemical reaction does not feed back on the hydrodynamic motion as the viscosity of the two solutions at hand is not influenced by the reactions. Recently, reaction driven viscosity changes have been shown numerically to lead to new spatiotemporal dynamics of viscous fingering in chemical bistable autocatalytic systems providing traveling fronts between solutions of different viscosity.[6–8] Unfortunately the predicted nonlinear dynamics have not been observed to date mainly because autocatalytic reactions are usually performed in aqueous solutions for which the viscosity hardly changes with concentrations of solutes. The only striking evidence of chemically driven viscous fingering for miscible autocatalytic systems occurs in polymeric systems where the monomer solution and the polymer matrix can have quite strong differences in viscosity.[9]

In miscible systems, chemical reactions are more prone to provide density differences that can drive buoyantly unstable situations as soon as a heavier fluid lies on top of a lighter one. Experimental evidence[10–20] and theoretical studies[20–32] on density driven instabilities have shown that the coupling between buoyancy driven flows and chemical reactions can strongly affect the properties of the fingering instability. The coupling with chemical reactions has been addressed mainly concerning the stability of planar fronts with regard to Rayleigh–Taylor fingering. A prototype system in that respect is the iodate-arsenious acid (IAA) reaction. In this redox reaction involving the oxidation of arse-

a)Electronic mail: adewit@ulb.ac.be

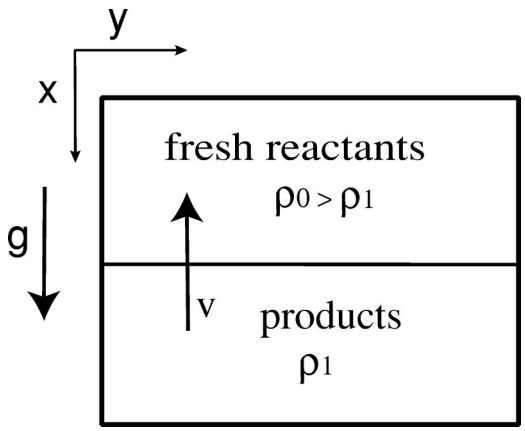

FIG. 1. Sketch of the system.

nous acid by iodate, traveling fronts between fresh reactants and products can easily be triggered in a capillary tube, Hele-Shaw cells, or porous media. As the density of the solution is decreasing in the course of reaction, ascending fronts are buoyantly unstable in the gravity field as they correspond to heavier reactants lying on top of lighter products (see Fig. 1). Experiments in capillary tubes[10–12] have shown that curved ascending fronts traveling with a speed higher than that of descending stable planar fronts are then observed. Theoretical work for such narrow geometry provides the critical radius of the tube above which the hydrodynamic instability can develop, and a discussion on whether axi- or non-axisymmetric modes should be observed at onset.[22–27] More recently, experiments in Hele-Shaw cells have shown that several fingers can develop in this geometry where the front is laterally extended.[16–18,20] Dispersion curves providing the growth rate of the fingers as a function of their wave number have been measured experimentally.[17,20] These dispersion curves characterizing the early stages of the instability are well reproduced theoretically by linear stability studies of models coupling the evolution equation for the flow to that of the concentration of the species ruling the density of the solution.[20,29–31] Little is known, however, on the long time dynamics of the fingers for such laterally extended Hele-Shaw cells. Experimentally, merging, fading, shielding, and tip splitting of fingers are observed[18] but no detailed quantitative characterization of this nonlinear dynamics has been provided yet. From a theoretical point of view, one can find in the literature nonlinear simulations of chemically driven density fingering of the IAA system and other monostable autocatalytic reactions.[25,26,28,32] Unfortunately, there again, no quantitative measurements characterizing the nonlinear transient and asymptotic dynamics are available. Such characterization of the nonlinear dynamics of miscible fingering has been performed in numerous articles devoted to pure viscous and density fingering.[33–39] It is of interest to have a quantitative idea on how chemical reactions can change such nonlinear properties of the fingers.

In this article, we perform a numerical study of the interplay between monostable autocatalytic chemical reactions and density driven fingering in porous media or thin Hele-Shaw cells. We analyze the nonlinear dynamics and in particular characterize asymptotic regimes in terms of various parameters of the problem such as the dimensionless width of the system corresponding to a Rayleigh number, the Damköhler number, and the speed and width of the front. We first introduce a theoretical model describing this instability. After analyzing the pure density fingering instability in the absence of chemical reactions, we next study density fingering of a chemical front in the monostable IAA reaction.

II. MODEL

A. Darcy–Boussinesq equations

Our model system is a two-dimensional porous medium or thin Hele-Shaw cell of length L_x and width L_y with the gravity field $\mathbf{g}$ oriented along x (see Fig. 1). In this system, a solution of density ρ_1 containing a solute in concentration c_1 lies under another solution miscible with it of density $\rho_0 > \rho_1$ and where the concentration of the solute ruling the density of the solution can be taken without loss of generality to be equal to zero. Let us first consider Darcy–Boussinesq equations:

$$\nabla \cdot \mathbf{u} = 0, \tag{1}$$

$$\nabla p = -\frac{\mu}{\kappa}\mathbf{u} + \rho(c)\mathbf{g}, \tag{2}$$

$$\rho(c) = \rho_1 + (\rho_0 - \rho_1)\left(1 - \frac{c}{c_1}\right), \tag{3}$$

$$\frac{\partial c}{\partial t} + \mathbf{u}\cdot\nabla c = D\nabla^2 c + f'(c), \tag{4}$$

where $\mathbf{u}=(u_x,u_y)$ is the velocity field. The viscosity μ, molecular diffusion coefficient D, and permeability κ are constant in space and time and p denotes the pressure. In thin Hele-Shaw cells, $\kappa = a^2/12$ where a is the gapwidth. $f'(c)$ is the dimensional kinetic scheme. In diluted solutions, the density depends linearly on the concentration with $\rho_0 = \rho(c=0) > \rho_1 = \rho(c=c_1)$.[29]

This problem has neither a characteristic speed (because there is no injection) nor a characteristic length. Hence to nondimensionalize the equations, we consider that viscosity and buoyancy forces have the same amplitude which defines a characteristic speed U as

$$U = \frac{\Delta\rho g \kappa}{\nu} \tag{5}$$

with $\Delta\rho = (\rho_0 - \rho_1)/\rho_0$ and $\nu = \mu/\rho_0$ is the kinematic viscosity. In addition, in the evolution equation for c, it is expected that convection balances diffusion suggesting the following characteristic length L_h and time τ_h scales:

$$L_h = \frac{D}{U}; \quad \tau_h = \frac{D}{U^2}. \tag{6}$$

Let us nondimensionalize Eqs. (1)–(4) scaling the velocity, length, and time by U, L_h, and τ_h. The pressure, density, and concentration are scaled, respectively, by $\mu D/\kappa$, ρ_0, and c_1. We define in addition a hydrostatic pressure

gradient as $\nabla p''=\nabla p'-\rho_1'\mathbf{i}_x$ where $\mathbf{i}_x$ is the unit vector along x. Dropping all the primes, the evolution equations for the dimensionless variables become then

$$\nabla\cdot\mathbf{u}=0, \tag{7}$$

$$\nabla p=-\mathbf{u}+(1-c)\mathbf{i}_x, \tag{8}$$

$$\frac{\partial c}{\partial t}+\mathbf{u}\cdot\nabla c=\nabla^2 c+f(c), \tag{9}$$

where $f(c)$ is now a dimensionless kinetic scheme. The dimensionless domain width of the system becomes

$$L_y'=\frac{L_y}{L_h}=\frac{L_y g\kappa\Delta\rho}{\nu D}=Ra, \tag{10}$$

where the dimensionless parameter Ra corresponds to a Rayleigh number. Analogously, $L_x'=L_x g\kappa\Delta\rho/\nu D=A\ Ra$ where A is the aspect ratio of the system. Taking the curl of (8) and introducing the stream function ψ such that $u=\partial\psi/\partial y$ and $v=-\partial\psi/\partial x$, we obtain the final dimensionless equations:

$$\nabla^2\psi=-c_y, \tag{11}$$

$$\frac{\partial c}{\partial t}+c_x\psi_y-c_y\psi_x=\nabla^2 c+f(c), \tag{12}$$

where the subscripts denote partial derivatives.

B. Reaction-diffusion front

As a model system, we consider a simple one-variable cubic kinetics capable of sustaining traveling fronts between a kinetically stable and an unstable state when coupled to molecular diffusion. This chemical model has been studied in detail theoretically and accounts quantitatively for experiments performed with the iodate-arsenious acid (IAA) redox reaction in some parameter range.[20,29–31,40] In the absence of flow, its dynamics follows the dimensional reaction-diffusion evolution equation:[41]

$$\frac{\partial c}{\partial t}=D\nabla^2 c-qc(c-c_1)(c+c_2) \tag{13}$$

with $c=[I^-]$, $c_1=[IO_3^-]_o$, $c_2=k_a/k_b$, $q=k_b[H^+]^2$ where k_a and k_b are kinetic constants. Following the reasoning of Sec. II A, we introduce new dimensionless variables $x'=xU/D$, $y'=yU/D$, $\tau'=tU^2/D$, $c'=c/c_1$. In terms of these variables, Eq. (13) can be written after omitting the primes:

$$\frac{\partial c}{\partial t}=\nabla^2 c-Dac(c-1)(c+d) \tag{14}$$

with

$$Da=\frac{Dqc_1^2}{U^2},\quad d=\frac{k_a}{k_b c_1}. \tag{15}$$

Da is the ratio τ_h/τ_c between the characteristic hydrodynamic time scale $\tau_h=D/U^2$ and the chemical time scale $\tau_c=1/qc_1^2$, i.e., Da is the Damköhler number of the problem. The higher the Damköhler number, the quicker the chemical time scale and hence the stronger the chemical effects with regard to the hydrodynamic effects. The $c=1$ solution is the kinetically stable chemical steady state corresponding to the final products while $c=0$ corresponds to the unstable fresh reactants. Equation (14) admits as solution the following propagating front:[29,41,42]

$$c(x,t)=\frac{1}{1+e^{k(x-vt)}}=\frac{1}{2}\left[1+\tanh\left(-\frac{k}{2}(x-vt)\right)\right] \tag{16}$$

where $k=\sqrt{Da/2}$. This planar front travels with a speed v equal to

$$v=\sqrt{\frac{Da}{2}}(1+2d). \tag{17}$$

The width w of the planar chemical front arbitrarily defined as the distance between $c=\delta$ and $c=1-\delta$ can readily be found from (16) to be equal to

$$w=\sqrt{\frac{8}{Da}}\ln\left(\frac{1-\delta}{\delta}\right). \tag{18}$$

Expressions (17) and (18) show thus that increasing Da leads to sharper fronts traveling with a higher speed. Let us note here that the chemical front defined by (16) corresponds to a kinetically stable steady state ($c=1$) invading an unstable steady state ($c=0$) with a constant speed v and width w resulting from the sole combination of autocatalytic reaction and diffusion. Such a front is different from the stationary front between two stable steady states (obtained for a bistable kinetics) the viscous and density fingering of which has been analyzed in Refs. 6, 7, and 43, respectively.

III. NUMERICAL SCHEME AND VALIDATION STUDIES

Let us now analyze the nonlinear fingering dynamics of the chemical front (16) when buoyancy effects are destabilizing. To do so, we numerically integrate the following model:

$$\nabla^2\psi=-c_y, \tag{19}$$

$$\frac{\partial c}{\partial t}+c_x\psi_y-c_y\psi_x=\nabla^2 c-Dac(c-1)(c+d). \tag{20}$$

Our pseudospectral numerical scheme is based on that developed by Tan and Homsy[34] and modified to take the chemical scheme into account. The linear terms of Eqs. (19) and (20) are computed in Fourier space. The nonlinear terms are calculated in real space. Back and forth between real and Fourier spaces are done using fast Fourier transforms from the FFTW library. The time-stepping scheme is a second order Adams–Bashforth scheme. The spatial discretization (unless stated otherwise) uses a ratio of 4 between the number of spectral modes CELY and CELX and the dimensionless width $L_y'=Ra$ and length $L_x'=ARa$. In other words, the spatial discretization step $dx=L_x'/\mathrm{CELX}=4$ and similarly $dy=L_y'/\mathrm{CELY}=4$. The corresponding time step is $dt=0.2$. As initial conditions, we choose $\psi=0$ everywhere which corresponds to solutions initially convectively at rest. For the concentration, we take as an initial condition either a step function between $c=1$ and $c=0$ or the analytical front function (16) located close to the upper boundary and the reverse step

or front function at the bottom of the system. The upper front corresponds to the lighter $c=1$ product solution invading downdards into the heavier $c=0$ reactant solution which, in a gravity field, corresponds to a buoyantly stable planar front traveling with velocity v and width w given by (17) and (18), respectively. The reverse upwards moving front is on the contrary buoyantly unstable and develops fingering. Periodic boundary conditions are used in both longitudinal and transverse directions. While using periodic boundary conditions in the transverse direction is quite standard, considering periodic boundary conditions in the streamwise direction implies to use the above described periodic extension of the displacement front to avoid Gibb's phenomena. As has been shown in many previous studies (see, for example, Refs. 34, 35, 37, 44, and the references therein), use of such boundary conditions place only a limit on the maximum time of the simulation (reached when the two counterpropagating fronts start to interact) but not on its accuracy. To initiate fingering, white noise of 0.1% in amplitude is added to the $c=0.5$ isolines in the initial step function of concentration. If the initial condition is the chemical front (16) then noise of 0.1% in amplitude is added on the concentration field in the area where $0.4<c<0.6$.

For buoyantly stable systems (i.e., $\nabla^2\psi=0$), the evolution of initial steps follows the standard error function, solution of the pure diffusive transport when $Da=0$ while for $Da\neq 0$, we recover the traveling front (16) with the correct speed (17) and width (18) dependence as a function of Da. For buoyantly unstable stratification, if $Da=0$, there is no chemical reaction and the model features pure density fingering. If $Da\neq 0$, we analyze then the effect of chemical reactions on density fingering. We have tested that, in these cases, the spatiotemporal fingering dynamics remains robust with regard to refinement of time and space discretization steps. In addition, we have checked for several values of parameters that the wavelength of the fingers that appear at early times is in good quantitative agreement with the value of the most unstable mode predicted by the linear stability analysis given in Ref. 29. As an example, for a system of width $Ra=2048$ and $Da=0.1$, $d=0.2$, the first visible pattern contains 27 fingers which appear at a dimensionless time of the order of $t=500$. This corresponds to a most unstable wave number $k=0.08$ and a growth rate $\sigma=0.013$ in quite good agreement with the value predicted by the linear stability analysis (see Fig. 3 of Ref. 29). The dynamics will be represented by two-dimensional density plots of the concentration ranging from $c=0$ (white) to $c=1$ (black)—see Fig. 2 for instance. The aspect ratio between x and y is preserved in the plots and the focus is put only on the dynamics of the unstable front.

IV. DENSITY FINGERING OF A CHEMICAL FRONT: NONLINEAR DYNAMICS

Figure 2 shows a typical simulation of pure density fingering without chemical reactions obtained for $Da=0$ and $Ra=512$. The nonlinear dynamics of pure density fingering has been analyzed in Hele-Shaw cells first experimentally by Wooding.[45] More recently, Fernandez *et al.* have performed

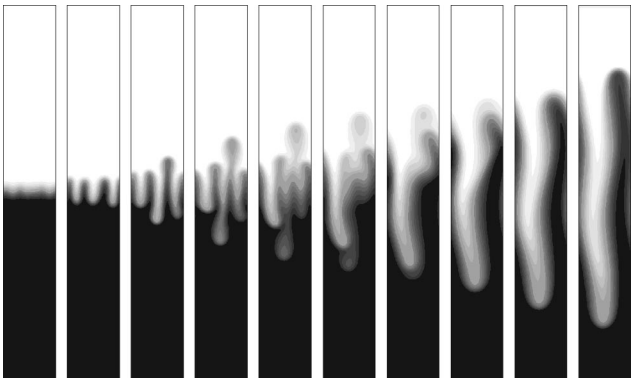

FIG. 2. Pure density fingering in the absence of chemical reactions, i.e., $Da=0$ shown from left to right from $t=2000$ up to $t=11\,000$ with a time interval of $\Delta t=1000$ in a system of dimensionless width $Ra=512$. Fingering conserves an up and down invariance with regard to the position of the initial front, i.e., the fingers elongate on average as far upwards and downwards in the course of time.

in the same geometry well controlled experiments characterizing such Rayleigh–Taylor instability in the linear regime[46] and have compared their results with theoretical stability analysis achieved in Refs. 47 and 48. The nonlinear dynamics of fingering is known to be characterized by merging and shielding[33,38,39] leading to an overall coarsening of the fingers.[49] Tip splittings are observed in larger systems.[38,45] Pure density fingering is invariant with respect to the change of variable $x\rightarrow -x$, $u_x\rightarrow -u_x$ as can be seen from Eqs. (7)–(9) where $f(c)=0$. This implies that, on average, fingers moving up and downwards have the same length with regard to the position of the initial front for a given time,[38,46] a property that we will call here up and down invariance.

This purely hydrodynamic fingering must be contrasted with fingering in the presence of chemical reactions shown in Fig. 3 for different values of Da and d with $Ra=512$. Clearly the chemical reaction breaks the up and down invariance because of the influence of the front velocity. As the front is moving upwards, fingers growing downwards are advected and impaired. This results in the eating of the white fingers corresponding to the kinetically unstable $c=0$ state by the black stable $c=1$ solution. Comparison of Figs. 2 and 3 enlightens the asymptotic dynamics for pure and reactive fingering, respectively. For $Da=0$ (Fig. 2), the fingers never stop elongating. For $Ra=512$, coarsening leads to one single finger which continues to extend in the course of time. Chemical reactions drastically change this picture. The asymptotic dynamics is still one single finger but its longitudinal extent is constant in time as a result of the competition between hydrodynamic convection which creates and stretches the finger and chemical reactions which favor planar fronts. The characterization of the nonlinear dynamics can benefit from various types of measurements[34–39,50] which we now present.

A. Averaged profiles

At successive times, the two-dimensional concentration field $c(x,y,t)$ can be spatially averaged along either the longitudinal x or transverse y coordinate to yield one-

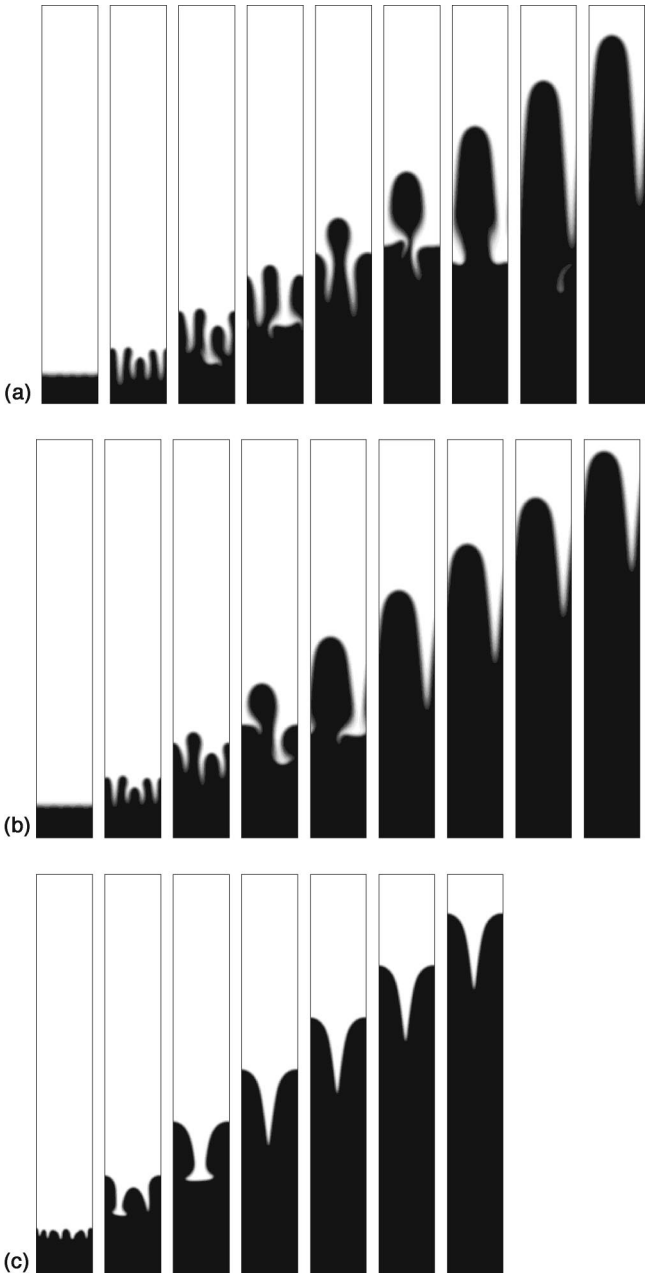

FIG. 3. Density fingering in the presence of chemical reactions shown from left to right from $t=1000$ up to $t=9000$ with a time interval of $\Delta t=1000$ in a system of dimensionless width $Ra=512$ with (from top to bottom lines) (a) $Da=0.01$, $d=0.01$; (b) $Da=0.01$, $d=0.3$; and (c) $Da=0.05$, $d=0.01$. The asymptotic dynamics is one single finger of fixed shape spanning the whole width of the system. Increasing Da at fixed d leads to more unstable fronts, i.e., earlier appearance of fingers with smaller wavelengths and to a final single finger of smaller extent traveling faster. Increasing d at fixed Da has little influence on the characteristics of the fingers at early times but later on leads to more rapid coarsening and a smaller final mixing zone.

dimensional averaged profiles. The transverse averaged profile

$$\langle c(x,t)\rangle=\frac{1}{L_y'}\int_o^{L_y'} c(x,y,t)dy$$

corresponds to standard curves computed in fingering studies. If the traveling front is stable, we recover in this transverse profile the front solution (16). As soon as fingering starts, bumps appear in $\langle c(x,t)\rangle$ as can be seen in Fig. 4 which shows the transverse averaged profiles as a function of time corresponding to the nonlinear dynamics of Fig. 3(a). The transverse profiles witness also the asymptotic finger which appears as a deformed traveling front moving with a constant shape and speed. The longitudinal averaged profiles

$$\langle c(y,t)\rangle=\frac{1}{L_x'}\int_o^{L_x'} c(x,y,t)dx$$

allows one to follow the interaction between fingers and in particular shows clearly how fingers interact, can spread and shield their neighbors, or merge to ultimately lead to one asymptotic single finger (Fig. 5).

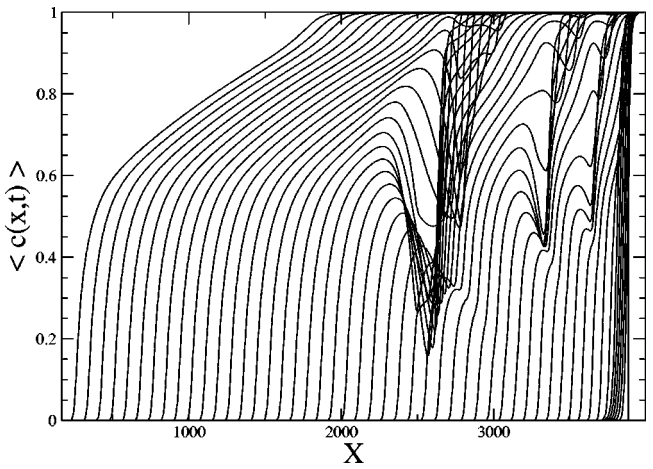

FIG. 4. Transverse averaged profiles $\langle c(x,t)\rangle$ for the simulations of Fig. 3(a) for $Ra=512$, $Da=0.01$, $d=0.01$. The time interval between two successive curves is $\Delta t=200$. The front travels from right (bottom of the setup) to left (top of the system).

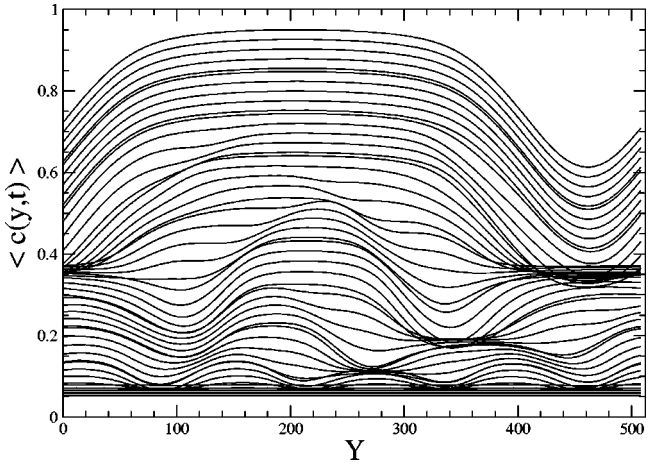

FIG. 5. Longitudinal averaged profiles $\langle c(y,t)\rangle$ for the simulations of Fig. 3(a) for $Ra=512$, $Da=0.01$, $d=0.01$. The time interval between two successive curves is $\Delta t=200$.

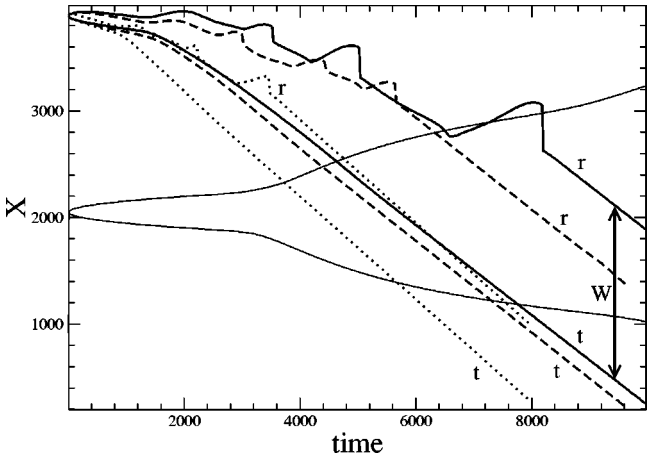

FIG. 6. Location of the tip (t) and the rear (r) of the fingering zone as a function of time for the simulations of Figs. 2 (full line) and 3: (a) $Da=0.01$, $d=0.01$: bold line; (b) $Da=0.01$, $d=0.3$: dashed line; and (c) $Da=0.05$, $d=0.01$: dotted line. When reaching the final asymptotic finger for $Da\neq 0$, the tip and rear travel at the same speed and are separated by a constant mixing zone W.

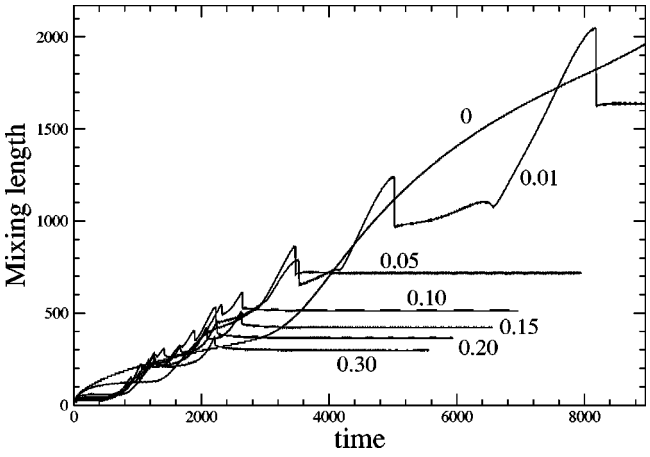

FIG. 7. Mixing length as a function of time for various values of the Damköhler number at fixed $d=0.01$ in a system of dimensionless width $Ra=512$.

B. Position of the tip and rear of the fingered zone

The transverse averaged profile is next used to define the tip and rear of the fingered zone. The tip is chosen arbitrarily as the location along the x axis in front of which the averaged concentration $\langle c(x,t)\rangle$ is less than $\delta=0.01$. The rear corresponds on the other hand to the location behind which $\langle c(x,t)\rangle$ is greater than 0.99. These points represent the most and least advanced locations of the fingered zone. Figure 6 shows the position of the tip and rear as a function of time for the four simulations of Figs. 2 and 3. The full line is the situation in the absence of chemical reactions ($Da=0$). The growth is symmetric with regard to the initial position of the front which is characteristic of the up and down invariance of the purely hydrodynamic density fingers. After an initial growth in $\sqrt{t}$ due to dispersive mixing of the two fluids, a linear growth follows as soon as fingering with several fingers sets in.[45] In narrow systems, if only one or two fingers remain present, the motion of tip and rear can depart from such a linear growth because of transverse diffusion[35,51] as seen in Fig. 6. In any case, the growth of the mixing zone is always continuous as the fingers keep stretching both up and downwards.

The bold, dashed, and dotted lines in Fig. 6 correspond to the situation in the presence of chemical reactions for various Da and d. The chemical reactions induce a breakdown of the up and down invariance due to the presence of the characteristic velocity of the front. Starting from an initial step function, the planar reaction-diffusion front establishes initially. The tip and rear move in parallel separated by a distance w [see Eq. (18)] as long as the front is not destabilized. They both travel at the same speed v [given by (17)] which is the speed of the stable traveling front obtained here as the slope of the linear initial transient. After a certain induction time which is a decreasing function of Da, the tip starts to move more quickly when fingering starts. In this fingering regime, the location of the tip varies linearly in time but with a quicker ''nonlinear'' speed V resulting from the nonlinear interaction between the convection rolls and the traveling front. V is measured by computing the slope of the curve at final times. The higher the Damköhler number, the higher this nonlinear speed. The rear of the front is entrained by the chemical front. The observed bumps correspond to the disappearance of the tail of white ($c=0$) fingers in the black ($c=1$) background as the traveling front is moving up (see in Fig. 3 the formation of little white tails into a black background and their sudden disappearance). After all fingers have merged and only one single finger remains, the rear travels then in parallel again with the tip at the nonlinear speed V. They are separated by a constant mixing zone of extent W, larger than the width w of the stable planar front.

C. Mixing length

The nonlinear dynamics of the fingers can typically be characterized by the mixing length defined as the distance between the tip and the rear of the fingers. The mixing lengths computed as a function of time for various Da keeping d fixed and starting from a step function are shown in Fig. 7. If $Da=0$, we recover the initial dispersive growth in $\sqrt{t}$ followed by the linear growth due to density fingering. When only one finger remains such as in Fig. 2 for $Ra=512$, Taylor dispersion can lead to departure from this linear growth at a later time. Nevertheless, the growth of the mixing zone is always continuous and monotonic. For $Da\neq 0$, the early time shows a constant mixing zone corresponding to the width of the stable front given by (18). After a certain induction time, fingering starts. The higher Da, the shorter the induction time and the higher the slope of the initial linear growth of the mixing length. This can be understood by the fact that, for higher Da, the width w of the front is smaller and hence the system is more unstable.[29] Nevertheless, as time goes by, it is observed that the nonlinear dynamics leads to much more effective coarsening of the fingers for higher Da. The fact that the tails of the downward moving fingers are entrained leads to a sudden abrupt decrease of the mixing zone corresponding to a very rapid movement of the rear of the fingered zone (see Fig. 6). Ul-

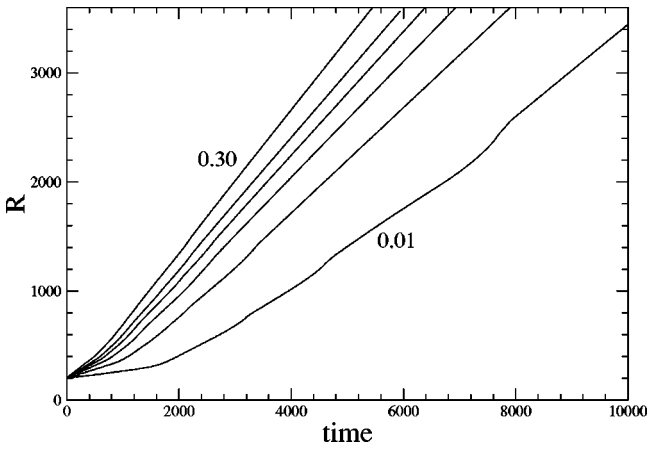

FIG. 8. Reaction rate R as a function of time for $Ra=512$, $d=0.01$ and the same various values of the Damköhler number as in Fig. 7, i.e., $Da=0.01$; 0.05; 0.1; 0.15; 0.20; 0.30 from the bottom up to the upper curve.

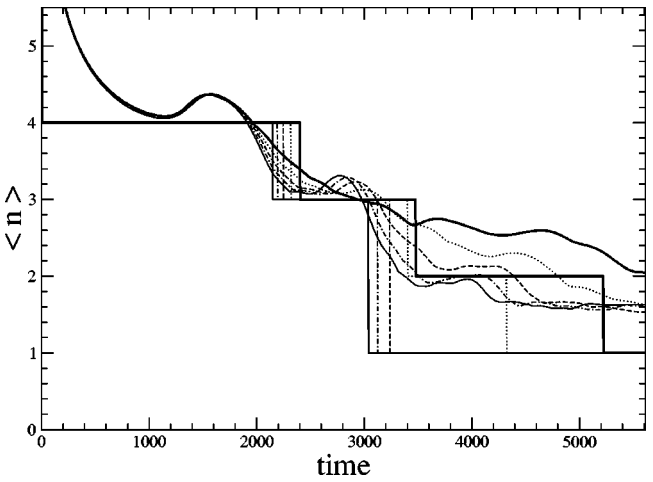

FIG. 9. Power averaged mean number $\langle n\rangle$ of fingers (continuous curves) in the system as a function of time for $Ra=512$, $Da=0.01$ and various values of $d=0.01$ (bold), 0.1 (dotted), 0.2 (dashed), 0.3 (dot-dashed), and 0.4 (plain). The stepped curves represent the Fourier mode with the highest amplitude as a function of time.

timately, there is saturation to a constant mixing zone of extent W characterizing the final single finger. Increasing Da gives less elongated fingers characterized by a smaller mixing zone W. This is due to the competing effects of hydrodynamic fingering and chemical reactions which for higher Da become more effective. As the pure reaction-diffusion front is planar, the higher Da (and hence the more effective the chemistry) the stronger the tendency to overcome fingering and hence the smaller the asymptotic mixing zone W.

D. Reaction rate *R*

If the chemical reactions affect the hydrodynamic fingering, fingering also has an influence on the reaction rate. Indeed in a fingered front, the contact zone between the two solutions is increased and it is expected that the reaction will speed up because of the convective movements of the fluid. In that respect, an interesting measure[52] is given by the reaction rate R computed in terms of the area of the reacted zone (i.e., the number of points where c is higher than an arbitrary threshold c^*) normalized by the width of the system versus time. In other words, we compute as a function of time the quantity

$$R(t)=\frac{1}{L_y'}\int_0^{L_x'}\int_0^{L_y'}\gamma dxdy, \tag{21}$$

where $\gamma=1$ if $c(x,y,t)>c^*$ and zero otherwise. The larger the contact zone between the two fluids, the higher the reaction rate. Figure 8 provides the reaction rate R as a function of time for the simulations of Fig. 7. R is by definition a function of the chosen threshold c^* but the slope of the curve $R(t)$ is independent of it and characterizes the average speed $\overline{V}$ of the fingers. $\overline{V}$ is thus here the rate of change of the area of the region where reaction has happened, normalized by the width of the channel. Because of convection, the average speed $\overline{V}$ is higher than the speed v of the stable planar chemical front. The average speed $\overline{V}$ measured as being the asymptotic slope of the function $R(t)$ is equal to the nonlinear speed V defined as the asymptotic slope of the location of the tip versus time. As an example, let us consider the results of Fig. 3. For $Da=0.05$ and $d=0.01$, the velocity v of the planar stable front is equal to 0.161 [see Eq. (17)] while $\overline{V}$ computed as the slope of the corresponding reaction rate R versus time (Fig. 8) is equal to 0.482, the same value V as the slope of the tip of the fingers versus time obtained in Fig. 6. The tip of the fingered zone travels thus with the same velocity as the whole fingered zone on average, this velocity being constant and larger than that of planar fronts. Such an enhancement of the velocity of chemical fronts due to convection has been observed for quite a long time in capillary tubes.[10,11]

E. Power averaged mean wave number

In the absence of tip splittings, the nonlinear dynamics of the system is clearly dominated by coarsening of the fingers both in the absence[49] and presence of chemical reactions. A convenient quantitative measure of this phenomenon is provided by the power averaged mean wave number[35] defined as

$$\langle k(t)\rangle=\frac{\Sigma_i k_i P_i}{\Sigma_i P_i}, \tag{22}$$

where k_i are the Fourier modes of the Fourier transform $\hat{c}(k,t)$ of the transverse averaged profile $\langle c(y,t)\rangle$ and $P(k)=|\hat{c}(k)|^2$ is their amplitude in Fourier space. The averaged wavelength of the fingers is thus simply $\langle\lambda(t)\rangle=2\pi/\langle k(t)\rangle$. Figure 9 shows the power averaged mean number of fingers in the system defined as $\langle n\rangle=Ra/\langle\lambda(t)\rangle$. As can be seen, this number decreases in time as a consequence of coarsening. When d is increased for fixed Da, coarsening is more efficient as $\langle n\rangle$ is smaller for a given time. Similar information is obtained by looking at the step-like function of Fig. 9 which represents simply the mode of maximum amplitude. One can clearly see that the system switches from four fingers in the width of the system to three, then two, and eventually one single finger for d

$=0.01$. For a higher value of $d=0.4$, the coarsening is more effective and the mode of highest amplitude switches directly from 3 to 1. A similar trend is observed when keeping d fixed and increasing Da, i.e., coarsening is more effective for higher Da.

F. Maxima and minima

A nice way to look at the dynamics of the system is to plot a space-time diagram of the locations of the maxima and minima of the transverse averaged profile $\langle c(y,t)\rangle$ in the course of time (see Fig. 10). Such a diagram enlightens the mechanism of shielding of one finger by its spreading neighbor and the subsequent reordering of the positions of the extrema until one ultimate single finger remains.

V. PARAMETRIC STUDY

The nonlinear dynamics is clearly influenced by the chemical reactions. Let us now analyze quantitatively to what extent variations of the three relevant parameters of the problem, i.e., the Rayleigh number Ra, the Damköhler number Da, and the chemical parameter d, influence the dynamics of the fingers.

At this stage, it is important to note that the initial condition of the simulation may have an influence on the transient nonlinear dynamics. If we start from a step function rather than from the traveling front solution (16), the initial width of the front is smaller and the system is more unstable.[29] Fingering starts thus earlier for a step initial condition than for a front of given extent. Nevertheless, in both cases, the asymptotic dynamics is the same single finger traveling with the same speed V and with the same mixing zone W.

The noise which seeds the initial condition is also quite important for the transient dynamics of the system going towards the final one single finger. Fingering starts indeed earlier when the noise has a higher amplitude. The number of fingers which appear out of the noise is, in any case, set up by the most unstable wave number given by the linear stability analysis. However, the location of these fingers along the y axis and their subsequent nonlinear interactions depend on the noise. Repeating the same simulations for fixed parameters and an ensemble of initial conditions with a noise of the same amplitude, one obtains each time a different initial pattern (although with the same number of initial fingers) which has its own nonlinear dynamics. If there is no reaction, this leads to an ensemble of variable mixing lengths as a function of time, the slopes of which are scattered around a mean value. The influence of a given noise is much more pronounced for smaller Ra. For $Ra=256$ where only two fingers appear initially, the slope of the mixing length as a function of time is much more sensitive to possible channeling. For some initial conditions, channeling is observed while it is not for other ones. For Ra roughly above 1024, there are enough fingers so that the scattering around the mean value of the slope becomes smaller. These trends remain when chemical reactions are present but affect only the transient towards the final one single finger. In other words, the number of bumps seen in the time dependence of the mixing length and their time of appearance depend on the initial condition. Nevertheless, whatever the initial condition and whatever the amplitude of the noise, the system always ends up with one single finger with the same characteristics, i.e., the same extent W and the same nonlinear velocity V. The only influence of the initial condition is on the lateral position of its maximum which can be at any place along y

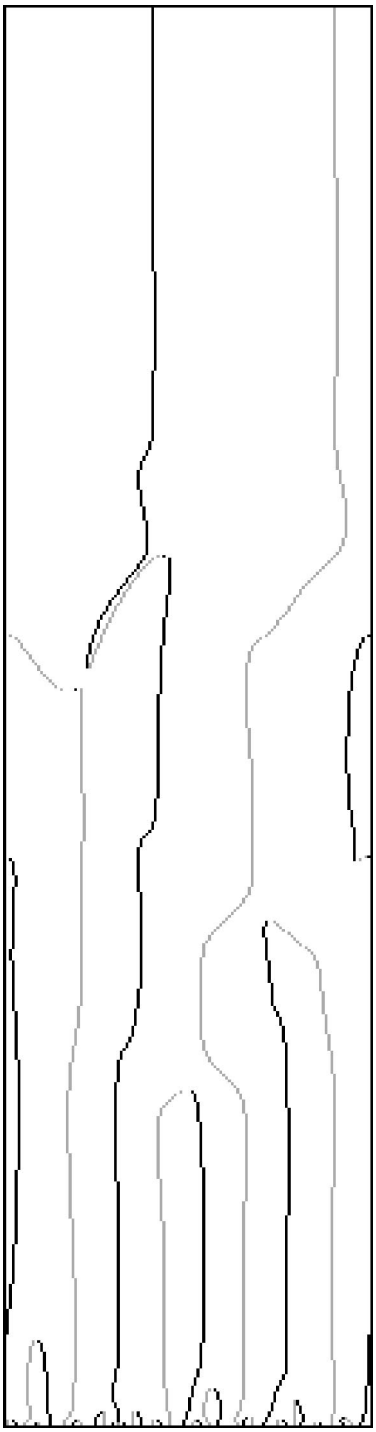

FIG. 10. Space-time map of the locations of the maxima (black) and minima (gray) of the transverse averaged profile $\langle c(y,t)\rangle$ as a function of time for simulation of Fig. 3(a) ($Ra=512$, $Da=0.01$, $d=0.01$). The horizontal direction corresponds to the y coordinate while the vertical axis is time running upwards.

as we use periodic boundary conditions along that direction. In that respect, all simulations presented in this article start from a step function with random noise of 0.1% in amplitude. Nevertheless, all asymptotic characteristics of the single finger presented in Figs. 11, 12, 16, and 17 are independent of the initial condition and of the amplitude of the noise.

A. Role of *d*

For the particular case of the IAA reaction, the kinetic parameter $d=k_1/k_2c_1$ can be varied by changing the initial concentration c_1 of the reactant. To be more general and draw conclusions that go beyond the peculiarities of the IAA model system, let us recall that d in fact influences the speed v of the stable planar front as $v=\sqrt{Da/2}(1+2d)$ but does not affect its width w. Increasing d leads thus to chemical fronts of constant width w traveling with an increased speed v. It has been shown on the basis of a linear stability analysis[29] that this leads to more stable fronts. An inspection of Figs. 3 and 9 and of other results for various Da and d shows that an increase of d merely affects the initial time of the nonlinear dynamics. The initial wavelength and time of appearance of the fingers depend very weakly on d but strongly on Da. The influence of d is, however, clear in the subsequent nonlinear dynamics of the fingers. Indeed, when d is increased, coarsening is more effective leading to more rapid merging of fingers and hence earlier reach of the asymptotic single finger. This single finger has a nonlinear speed V which is almost independent of d while its extension W is a decreasing function of d (see Fig. 11). This latter dependence is due to the fact that, for a higher chemical speed v, the displacement of the front is entraining more effectively fingering. The convection roll will thus be of smaller extent leading to smaller W. The nonlinear speed V is rather related to the amplitude of the velocity field which is a function of the density difference across the width w of the planar front. As w is independent of d, we can understand that V is almost independent of d. In real experiments, it is likely to be difficult to vary the speed v of a planar front without changing also its width w. In that respect, it is particularly instructive to look at the effect of Da on the dynamics.

B. Role of *Da*

The Damköhler number Da is the ratio between the hydrodynamic and chemical time scales. The higher Da, the more effective the chemistry. For planar reaction-diffusion fronts, increasing Da leads to sharper fronts traveling more quickly as can be seen by inspecting the Da dependence of v and w. A linear stability analysis shows that increasing Da, i.e., sharpening the front for a same density difference leads to more unstable fronts with regard to density fingering.[29] This is confirmed by nonlinear simulations [compare Figs. 2, 3(a) and 3(c)] which show that an increase of Da leads to the earlier appearance of fingers which have then smaller wavelengths. In addition, the higher Da, the more effective the coarsening. Indeed the asymptotic single finger is reached much more quickly for higher values of Da. This final finger

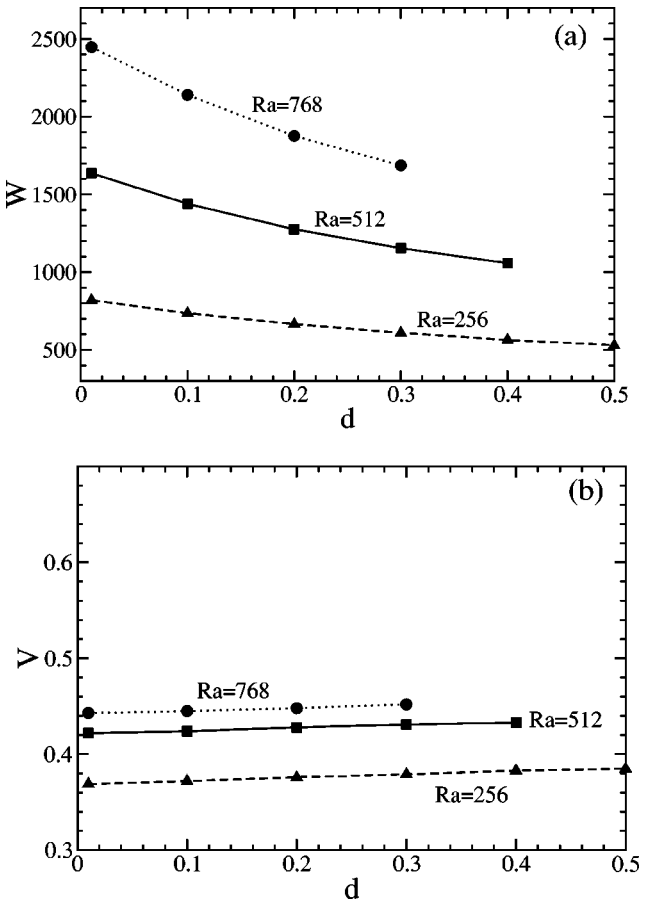

FIG. 11. Nonlinear mixing zone W (a) and speed V (b) of the asymptotic one single finger as a function of the parameter d for three values of Ra and $Da=0.01$.

is of smaller extent W and has a higher nonlinear speed V (see Fig. 12), a signature of the fact that chemistry is opposing more efficiently fingering. Let us note that the system is much more sensitive to changes in Da when Da is smaller than 0.1 and in particular when Da tends to zero. In other words, there is a huge difference between systems with and without chemistry but once chemistry is operative, there is a saturation of its effect when Da is further increased.

C. Role of *Ra*

In our scaling, Ra is the dimensionless width of the system. Increasing Ra thus simply leads to larger systems and hence to more fingers as, in our dimensionless variables, their wavelength is independent of Ra.[29] This can be seen when comparing simulations for the same Da and d but different Ra: Figures 3(a) and 3(c) for $Ra=512$ with Fig. 13 where $Ra=256$ and Fig. 14 where $Ra=2048$, all of them with $Da=0.01$ and 0.05 while $d=0.01$. Multiplying the width of the system by four roughly leads to four times as many fingers at early times. The nonlinear dynamics is nevertheless dependent on Ra. It is seen when comparing Figs. 3 and 13 at the same times that increasing Ra leads to a more rapid coarsening of the fingers. This is further testified by inspecting the Ra dependence of the mixing length for fixed Da and d (Fig. 15). In addition, when reaching an

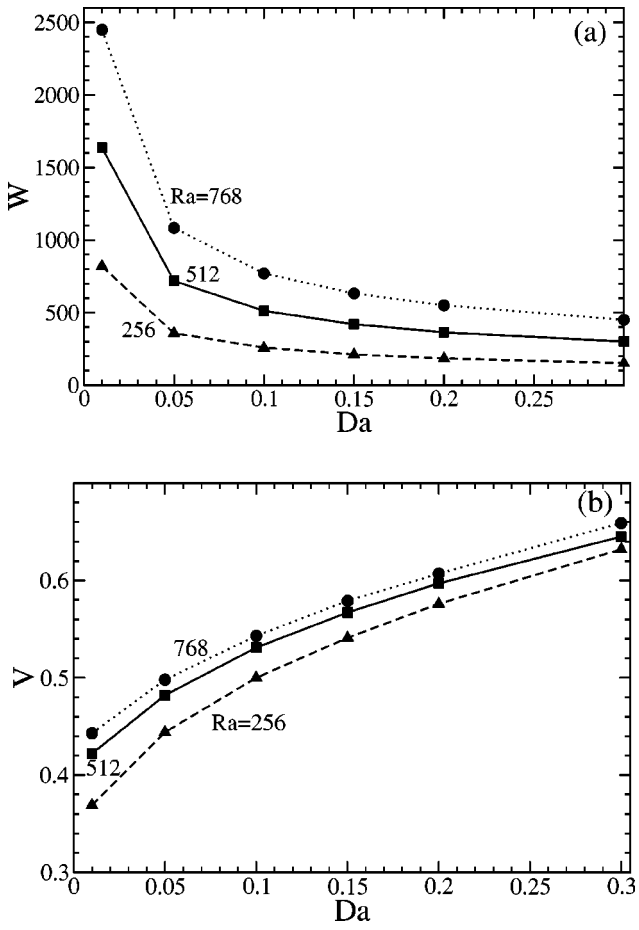

FIG. 12. Nonlinear mixing zone W (a) and speed V (b) of the asymptotic one single finger as a function of the parameter Da for three values of Ra and $d=0.01$.

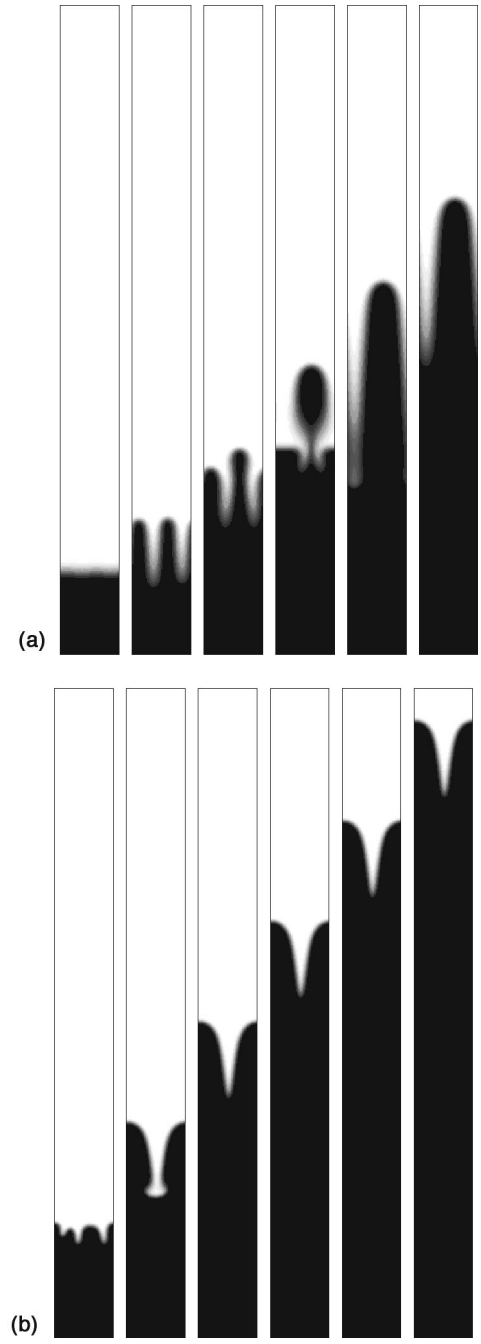

FIG. 13. Density fingering in the presence of chemical reactions. The upper and lower series correspond to $Da=0.01$ and $Da=0.05$, respectively, with $d=0.01$ and $Ra=256$. From left to right, the system is shown at successive times $t=1000$, 2000, 3000, 4000, 5000, and 6000.

asymptotic single finger, its width W and speed V are larger when Ra is larger (Figs. 11 and 12). This can be understood as in larger systems, the convection roll around the final single finger is of course larger for $Ra=512$ than for $Ra=256$ amplifying thus the effect of convection and hence stretching the finger.

Scaling laws can be extracted for the asymptotic single finger. Figure 16 represents the asymptotic mixing zone rescaled by Ra both as a function of Da and d. It is striking to see that the three curves $W/Ra=f(Da)$ fall exactly on the same curve which scales as $W/Ra=0.32/\sqrt{Da}$. The collapse on one single curve for $W/Ra=f(d)$ is better for $d\to 0$ which is interesting as in experimental conditions, $d=0.0021$.[29] No straightforward scaling came to us for V.

For what concerns the asymptotic profile, a comparison of Figs. 3 and 13 for the same Da and d show that the final finger shape for $Ra=512$ and 256 (as well as that for $Ra=768$ not shown here) are geometrically similar. In length scales rescaled by Ra, i.e., in units L_x'/Ra and L_y'/Ra, the axial and transverse averaged profiles of the final finger do indeed overlap (see Fig. 17) showing that the asymptotic fingers for different Ra but fixed Da and d are self-similar. In a coordinate system moving with speed V, the averaged profiles are therefore a stationary solution of the set of nonlinear equations. This suggests that one-dimensional front evolution equations would be sufficient to describe here the two-dimensional dynamics.[53]

It is known that in pure fingering phenomena, tip splittings may occur if the front has spread wide enough to allow more fingers to grow.[45] Hence tip splitting of density or viscous fingers is shown to appear beyond a given value of the dimensionless width of the system for a fixed density or viscosity ratio.[34,35,38] The same trend is observed with chemical reactions as can be seen in Fig. 18 where tip splittings of reactive fingers are observed for $Ra=5120$. So, it is expected that above a given critical Ra function of Da, the

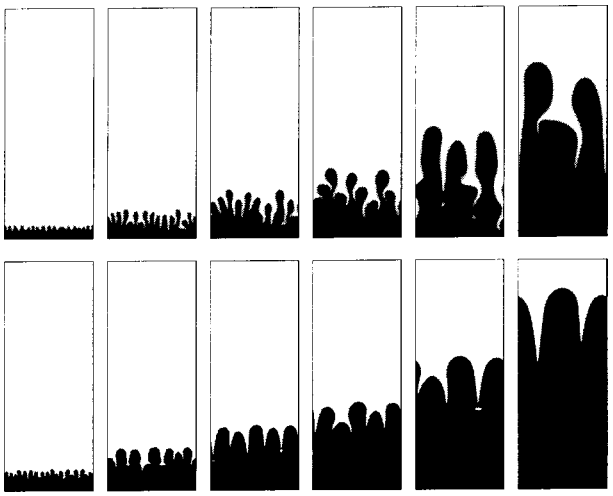

FIG. 14. Density fingering in the presence of chemical reactions. The upper and lower series correspond to $Da=0.01$ and $Da=0.05$, respectively, with $d=0.01$ and $Ra=2048$. From left to right, the system is shown at successive times $t=1000$, 2000, 3000, 4000, 6000, and 9000.

system will not evolve towards the asymptotic single finger but that large fingers will split again. As such simulations of large systems are very much time consuming, no detailed study of such tip splitting dynamics has been undertaken.

VI. CONCLUSIONS AND PERSPECTIVES

We have shown that chemical reactions can profoundly affect the nonlinear dynamics of density fingering of monostable chemical fronts. Our nonlinear simulations have been done using Darcy's law coupled to a reaction diffusion system with cubic kinetics allowing as a solution convectionless planar traveling fronts of concentration c. When the density of the solution depends on the concentration c of the solute, density fingering develops when the heavier solution lies on top of the lighter one. Monostable chemical reactions break the up and down ''invariance'' of the pure Rayleigh–Taylor fingering leading to a competition between the hydrodynamic instability that favors monotonic extension of the convection and chemistry that prefers traveling planar flat fronts. In systems of small lateral extent, this competition leads to one final single finger traveling with a nonlinear speed V larger than the velocity v of the planar front and having an extension $W>w$ where w is the width of the stable traveling front. The axial and transverse averaged profiles of the asymptotic final finger are shown to be self-similar for different Ra such that their mixing zone scales as $W/Ra \sim Da^{-0.5}$. In larger systems, tip splittings of the fingers are observed. This nonlinear dynamics has to be contrasted with that of fingering of bistable chemical systems leading to droplet formation.[43]

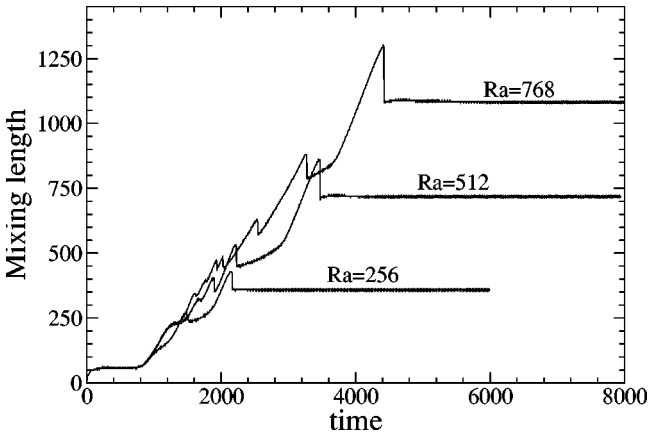

FIG. 15. Mixing lengths for $Da=0.05$, $d=0.01$ and various Ra.

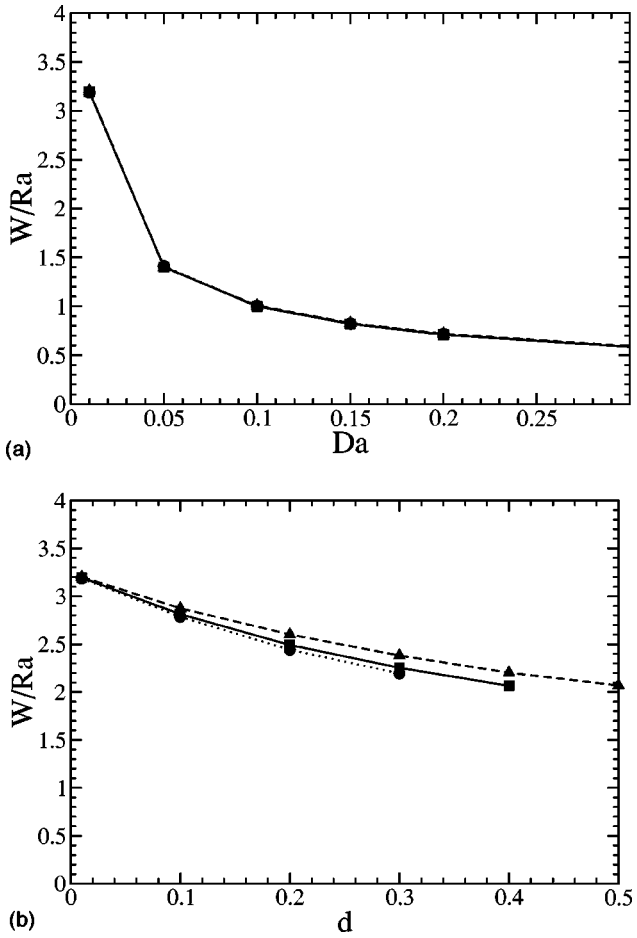

FIG. 16. Asymptotic mixing zone W of the final finger normalized by the Rayleigh number Ra as a function of Da (a) and d (b) for three values of Ra (dashed: $Ra=256$; plain: $Ra=512$; dotted: $Ra=768$). The three curves in (a) all match the function $W/Ra=0.32/\sqrt{Da}$.

The cubic scheme used here accounts quantitatively for the monostable IAA reaction in some parameter range. The conclusions gained using the IAA reaction are nevertheless very general and could apply to any reaction-diffusion front for which one kinetically stable steady state invades an unstable one. Indeed any traveling front is characterized by an intrinsic speed v and width w that depend here on the parameters d and Da specific for the IAA system. As our discussion goes beyond the peculiar value of the parameters Da and d to reach an understanding in terms of the effect of increasing the speed v and width w of the front, these conclusions should remain valid for any other chemical front subject to density fingering. In particular, we have shown that fronts traveling faster will undergo a much more effec-

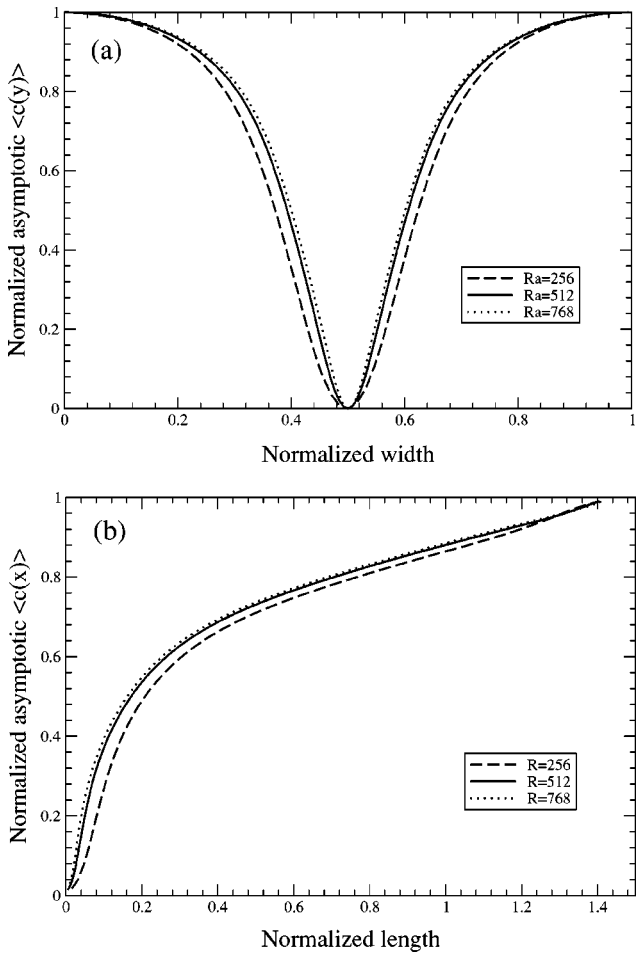

FIG. 17. Superposed axial (a) and transverse (b) asymptotic averaged finger profiles for three different values of Ra on length scales normalized by Ra for $Da=0.05$ and $d=0.01$.

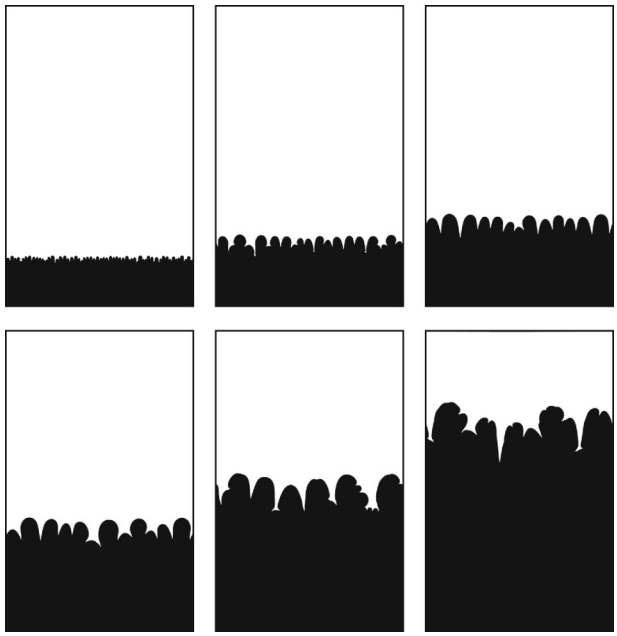

FIG. 18. Tip splittings observed in large systems with $Ra=5120$, $d=0.0021$, $Da=0.1$ and $dx=dy=10$. From left to right and top to bottom, the system is shown at successive times $t=1000$, 2000, 3000, 4000, 6000, and 9000.

tive coarsening leading more quickly to a final finger of smaller extent because quicker fronts oppose much more efficiently to the convective rolls set up by a fixed density difference across the front. Similarly, sharpening the fronts makes them more unstable and undergo quicker coarsening which, in smaller systems, leads to one single finger of decreasing W and increasing V. Such conclusions should be independent of the details of the kinetics. This is further suggested by the fact that analogous preliminary trends (and in particular the asymptotic single finger) have been obtained in a study of density fingering of another front producing monostable autocatalytic reaction: the chlorite-tetrathionate (CT) system.[32]

This work calls for further extensions. First of all, comparisons with experimental results made with buoyantly unstable IAA fronts or other autocatalytic reactions in porous media or thin Hele-Shaw cells would be welcome. From a theoretical point of view, it would be of interest to analyze in detail to what extent the nonlinear dynamics described here are robust with regard to changes in the hydrodynamics or in the chemical kinetics. Concerning the hydrodynamics, linear stability analysis have shown that the use of 2D Brinkman's or 3D Stokes equations for Hele-Shaw cells of larger gap-widths changes quantitatively but not qualitatively dispersion curves with regard to a Darcy description.[20,30,31] The question raised now is whether such a conclusion can be extended to the nonlinear regime as well.[54] In other words, would nonlinear dynamics such as the switch from one asymptotic self-similar single finger towards tip splittings when the dimensionless width of the domain is increased or the more effective coarsening induced by increasing the speed of the front or sharpening its width be robust with regard to three-dimensional effects? Could any new dynamics come into play? What would the scaling laws concerning the asymptotic finger (if robust) be in 3D? Concerning the chemical kinetics, while nonlinear simulations using a one-variable chemical scheme of order four modeling the CT reaction have shown that one single finger can also be recovered,[32] a more detailed analysis of the nonlinear speed V and mixing zone W as a function of the parameters would now be welcome. In particular, in some parameter range, the CT reaction is better described by a two-variable model and variation of the ratio of molecular diffusivities of the important chemical species could quantitatively affect the dynamics as well. Moreover, in some cases, the exothermicity of the reaction cannot be neglected and the nonlinear dynamics is influenced as well by the heat released in the front.[55] Finally, from a mathematical point of view, characterization of the self-similar asymptotic profiles using nonlinear analytical techniques would be of great elegance.

ACKNOWLEDGMENTS

The author thanks F. Otto for fruitful discussions as well as FRFC (Belgium), Prodex, and ESA for financial support. A.D. is a Research Associate at the FNRS (Belgium).

[1]J. Chadam, D. Hoff, E. Merino, P. Ortoleva, and A. Sen, ''Reactive infiltration instabilities,'' IMA J. Appl. Math. **36**, 207 (1986).
[2]H. A. Nasr-El-Din, K. C. Khulbe, V. Hornof, and G. H. Neale, ''Effects of interfacial reaction on the radial displacement of oil by alkaline solutions,'' Rev. Inst. Fr. Pet. **45**, 231 (1990).
[3]M. Sastry, A. Gole, A. G. Banpurkar, A. V. Limaye, and S. B. Ogale, ''Variation in viscous fingering pattern morphology due to surfactant-mediated interfacial recognition events,'' Curr. Sci. **81**, 191 (2001).
[4]J. Fernandez and G. M. Homsy, ''Viscous fingering with chemical reaction: Effect of in-situ production of surfactants,'' J. Fluid Mech. **480**, 267 (2003).
[5]Y. Nagatsu and T. Ueda, ''Effects of reactant concentrations on reactive miscible viscous fingering,'' AIChE J. **47**, 1711 (2001).
[6]A. De Wit and G. M. Homsy, ''Viscous fingering in reaction-diffusion systems,'' J. Chem. Phys. **110**, 8663 (1999).
[7]A. De Wit and G. M. Homsy, ''Nonlinear interactions of chemical reactions and viscous fingering in porous media,'' Phys. Fluids **11**, 949 (1999).
[8]P. Grosfils and J.-P. Boon, ''Viscous fingering in miscible, immiscible and reactive fluids,'' Int. J. Mod. Phys. B **17**, 15 (2003).
[9]J. A. Pojman, V. M. Ilyashenko, and A. M. Khan, ''Free-radical frontal polymerization: Self-propagating thermal reaction waves,'' J. Chem. Soc., Faraday Trans. **92**, 2824 (1996).
[10]I. Nagypál, G. Bazsa, and I. R. Epstein, ''Gravity-induced anisotropies in chemical waves,'' J. Am. Chem. Soc. **108**, 3635 (1986).
[11]J. A. Pojman, I. R. Epstein, T. J. McManus, and K. Showalter, ''Convective effects on chemical waves. 2. Simple convection in the iodate-arsenous acid system,'' J. Phys. Chem. **95**, 1299 (1991).
[12]J. Masere, D. A. Vasquez, B. F. Edwards, J. W. Wilder, and K. Showalter, ''Nonaxisymmetric and axisymmetric convection in propagating reaction-diffusion fronts,'' J. Phys. Chem. **98**, 6505 (1994).
[13]C. R. Chinake and R. H. Simoyi, ''Fingering patterns and other interesting dynamics in the chemical waves generated by the chlorite-thiourea reaction,'' J. Phys. Chem. **98**, 4012 (1994).
[14]K. Eckert and A. Grahn, ''Plume and finger regimes driven by an exothermic interfacial reaction,'' Phys. Rev. Lett. **82**, 4436 (1999).
[15]D. Horváth, T. Bánsági, Jr., and A. Tóth, ''Orientation-dependent density fingering in an acidity front,'' J. Chem. Phys. **117**, 4399 (2002).
[16]M. R. Carey, S. W. Morris, and P. Kolodner, ''Convective fingering of an autocatalytic reaction front,'' Phys. Rev. E **53**, 6012 (1996).
[17]M. Böckmann and S. C. Müller, ''Growth rates of the buoyancy-driven instability of an auto-catalytic reaction front in a narrow cell,'' Phys. Rev. Lett. **85**, 2506 (2000).
[18]M. Böckmann, O. Inomoto, and S. C. Müller (personal communication, 2003).
[19]T. Bánsági, Jr., D. Horváth, and Á. Tóth, ''Convective instability of an acidity front in Hele-Shaw cells,'' Phys. Rev. E **68**, 026303 (2003).
[20]J. Martin, N. Rakotomalala, D. Salin, M. Böckmann, and S. C. Müller, ''Gravitational instability of miscible fluids in a Hele-Shaw cell and chemical reaction,'' J. Phys. IV **11**, 99 (2001).
[21]J. A. Pojman and I. R. Epstein, ''Convective effects on chemical waves. 1. Mechanisms and stability criteria,'' J. Phys. Chem. **94**, 4966 (1990).
[22]B. F. Edwards, J. W. Wilder, and K. Showalter, ''Onset of convection for autocatalytic reaction fronts: Laterally unbounded systems,'' Phys. Rev. A **43**, 749 (1991).
[23]D. A. Vasquez, J. W. Wilder, and B. F. Edwards, ''Hydrodynamic instability of chemical waves,'' J. Chem. Phys. **98**, 2138 (1993).
[24]J. Huang, D. A. Vasquez, B. F. Edwards, and P. Kolodner, ''Onset of convection for autocatalytic reaction fronts in a vertical slab,'' Phys. Rev. E **48**, 4378 (1993).
[25]J. Huang and B. F. Edwards, ''Pattern formation and evolution near autocatalytic reaction fronts in a narrow vertical slab,'' Phys. Rev. E **54**, 2620 (1996).
[26]D. A. Vasquez, J. W. Wilder, and B. F. Edwards, ''Chemical wave propagation in Hele-Shaw cells and porous media,'' J. Chem. Phys. **104**, 9926 (1996).
[27]D. A. Vasquez and C. Lengacher, ''Linear stability analysis of convective chemical fronts in a vertical slab,'' Phys. Rev. E **58**, 6865 (1998).
[28]D. Zhang, W. R. Peltier, and R. L. Armstrong, ''Buoyant convection in the Belousov–Zhabotinsky reaction. II. Chemically driven convection and instability of the wave structure,'' J. Chem. Phys. **103**, 4078 (1995).
[29]A. De Wit, ''Fingering of chemical fronts in porous media,'' Phys. Rev. Lett. **87**, 054502 (2001).
[30]J. Martin, N. Rakotomalala, D. Salin, and M. Böckmann, ''Buoyancy-driven instability of an autocatalytic reaction front in a Hele-Shaw cell,'' Phys. Rev. E **65**, 051605 (2002).
[31]R. Demuth and E. Meiburg, ''Chemical fronts in Hele-Shaw cells: Linear stability analysis based on the three-dimensional Stokes equations,'' Phys. Fluids **15**, 597 (2003).
[32]J. Yang, A. D'Onofrio, S. Kalliadasis, and A. De Wit, ''Rayleigh–Taylor instability of reaction-diffusion acidity fronts,'' J. Chem. Phys. **117**, 9395 (2002).
[33]G. M. Homsy, ''Viscous fingering in porous media,'' Annu. Rev. Fluid Mech. **19**, 271 (1987).
[34]C. T. Tan and G. M. Homsy, ''Simulation of nonlinear viscous fingering in miscible displacement,'' Phys. Fluids **31**, 1330 (1988).
[35]W. B. Zimmerman and G. M. Homsy, ''Nonlinear viscous fingering in miscible displacement with anisotropic dispersion,'' Phys. Fluids A **3**, 1859 (1991).
[36]W. B. Zimmerman and G. M. Homsy, ''Viscous fingering in miscible displacements: Unification of effects of viscosity contrast, anisotropic dispersion, and velocity dependence of dispersion on nonlinear finger propagation,'' Phys. Fluids A **4**, 2348 (1992).
[37]A. Rogerson and E. Meiburg, ''Numerical simulation of miscible displacement processes in porous media flows under gravity,'' Phys. Fluids A **5**, 2644 (1993).
[38]O. Manickam and G. M. Homsy, ''Fingering instabilities in vertical miscible displacement flows in porous media,'' J. Fluid Mech. **288**, 75 (1995).
[39]M. Ruith and E. Meiburg, ''Miscible rectilinear displacements with gravity override. Part 1. Homogeneous porous medium,'' J. Fluid Mech. **420**, 225 (2000).
[40]J. H. Merkin and H. Sevcikova, ''Travelling waves in the iodate-arsenous acid system,'' Phys. Chem. Chem. Phys. **1**, 91 (1999).
[41]A. Hanna, A. Saul, and K. Showalter, ''Detailed studies of propagating fronts in the iodate oxidation of arsenous acid,'' J. Am. Chem. Soc. **104**, 3838 (1982).
[42]A. Saul and K. Showalter, ''Propagating reaction-diffusion fronts,'' in *Oscillations and Traveling Waves in Chemical Systems*, edited by R. J. Field and M. Burger (Wiley, New York, 1985), pp. 419–439.
[43]A. De Wit, P. De Kepper, K. Benyaich, G. Dewel, and P. Borckmans, ''Hydrodynamical instability of spatially extended bistable chemical systems,'' Chem. Eng. Sci. **58**, 4823 (2003).
[44]A. De Wit and G. M. Homsy, ''Viscous fingering in periodically heterogeneous porous media. II. Numerical simulations,'' J. Chem. Phys. **107**, 9619 (1997).
[45]R. A. Wooding, ''Growth of fingers at an unstable diffusing interface in a porous medium or Hele-Shaw cell,'' J. Fluid Mech. **39**, 477 (1969).
[46]J. Fernandez, P. Kurowski, P. Petitjeans, and E. Meiburg, ''Density-driven unstable flows of miscible fluids in a Hele-Shaw cell,'' J. Fluid Mech. **451**, 239 (2002).
[47]J. Fernandez, P. Kurowski, L. Limat, and P. Petitjeans, ''Wavelength selection of fingering instability inside Hele-Shaw cells,'' Phys. Fluids **13**, 3120 (2001).
[48]F. Graf, E. Meiburg, and C. Härtel, ''Density driven instabilities of miscible fluids in a Hele-Shaw cell: Linear stability analysis of the three-dimensional Stokes equation,'' J. Fluid Mech. **451**, 261 (2002).
[49]Y. Ben, E. A. Demekhin, and H.-C. Chang, ''A spectral theory for small-amplitude miscible fingering,'' Phys. Fluids **14**, 999 (2002).
[50]J. C. Bacri, N. Rakotomalala, D. Salin, and R. Wouméni, ''Miscible viscous fingering-experiments versus continuum approach,'' Phys. Fluids A **4**, 1611 (1992).
[51]R. L. Slobod, E. J. Burcik, and B. H. Cashdollar, ''The effect of viscosity ratio and path length in miscible displacement in porous media,'' Prod. Mon. **20**, 11 (1959).
[52]P. Constantin, A. Kiselev, A. Oberman, and L. Ryzhik, ''Bulk burning rate in passive-reactive diffusion,'' Arch. Ration. Mech. Anal. **154**, 53 (2000).
[53]F. J. Fayers, ''An approximate model with physically interpretable parameters for representing miscible viscous fingering,'' SPERE Trans. AIME **285**, 551 (1988).
[54]B. F. Edwards, ''Poiseuille advection of chemical reactions fronts,'' Phys. Rev. Lett. **89**, 104501 (2002).
[55]T. Bánsági, Jr., D. Horváth, Á. Tóth, J. Yang, S. Kalliadasis, and A. De Wit, ''Density fingering of an exothermic autocatalytic reaction,'' Phys. Rev. E. **68**, 055301(R) (2003).